Real time simulation of MPPT algorithms for PV energy system

Bounechba, Hadjer; Bouzid, Aissa; Snani, Hamza; Lashab, Abderezak

Published in:
International Journal of Electrical Power & Energy Systems

DOI (link to publication from Publisher):
10.1016/j.ijepes.2016.03.041

Publication date:
2016

Document Version
Accepted author manuscript, peer reviewed version

Electrical Power and Energy Systems

Real time simulation of MPPT algorithms for PV energy system

Hadjer Bounechba, Aissa Bouzid, Hamza Snani, Abderezak Lashab

Laboratoire d'électrotechnique de Constantine, Département d'électrotechnique, Université Constantine 1, 25000 Constantine, Algeria

Keywords:
MPPT
Photovoltaic system
CPA
FSCC
dSPACE

A B S T R A C T

Solar panels have a nonlinear voltage-current characteristic, with a distinct maximum power point (MPP), which depends on the environmental factors, such as solar irradiance and ambient temperature. In order to increase the power extracted from the solar panel, it is necessary to operate the photovoltaic (PV) system at the maximum power point (MPP). In this paper a novel maximum-power-point tracking (MPPT) method based on current perturbation algorithm (CPA) with a variable perturbation step and fractional short circuit current algorithm (FSCC) to determine an optimum operating current. An exper-imental comparative study of these maximum power point tracking methods using dSPACE is presented in this article. The effectiveness of proposed algorithm in terms of dynamic performance and improved stability is validated by detailed simulation and experimental studies.

Introduction

Electricity production using non-conventional energy (oil, gas, ...) leads to the depletion of its reserves and intensifies the release of greenhouse gases and thus the pollution of the atmosphere resulting climate change. Faced with these alarming consequences, it was necessary to consider the development of alternative energy called renewable energy sources.

Solar energy is considered today as one of the most useful sources of renewable energy, because it is relatively less polluted and maintenance, an inexhaustible source, free and superabundant, looks very promising, available in every country and every day.

The disadvantage of the solar energy is that the sun doesn't shine 24 h a day, when the sun goes down or is heavily shaded, solar PV panels stop producing electricity. In addition, solar energy conversion efficiency into electrical energy is very low especially in low radiation areas.

Because of the non-linear relationship between the current and the voltage of the photovoltaic cell, it can be observed that there is a unique maximum power point (MPP) at a particular environment, and this peak power point keeps changing with solar irradiance and ambient temperature [1]. Therefore, monitoring of maximum power point tracking (MPPT) is an essential part of the photovoltaic (PV) system to ensure that the power converters operate at maximum power point (MPP) of the solar panel.

Many MPPT algorithms have been developed in [2,3]. These algorithms differ from each other in terms of number of the sensors used, complexity, and cost to implement the algorithm. The goal of all major MPPT algorithms is how to reach the maximum power quickly, with accuracy and especially reduce the disturbance around the MPP. Each algorithm can be categorized based on the type of the control variable it uses: (1) voltage; (2) current; or (3) duty cycle [4].

Among the more popular ones are perturb and observe (P&O) [5,6], incremental conductance (INC) [7], fractional open-circuit voltage (FOCV) [8] and fractional short-circuit current (FSCC) [9].

In the P&O method, a small perturbation (step size) is applying to control parameter and measures the PV array output power before and after the perturbation. If the power increases, the algorithm continues to perturb the system in the same direction; otherwise, the system is perturbed in the opposite direction.

In the INC method, operation point of module is determined which side of MPP by derivation of power to voltage and then, this point towards to MPP via tuning duty cycle. Both methods are working effectively under uniform irradiance because of only one MPP formed in this condition [10]. However, both P&O and INC methods always produce power loss oscillations around MPP in static weather and did not perform well during rapid changing of atmospheric conditions because of the MPP point vary with irradiance level and temperature.

Fast-changing solar irradiation level has a significant impact on the electrical characteristics than the temperature which usually changes quite slowly during the day, so that the temperature is often considered constant. Therefore, the effect of temperature on photovoltaic module performance is often neglected.

E-mail address: hadjer.bounechba@lec-umc.org (H. Bounechba).

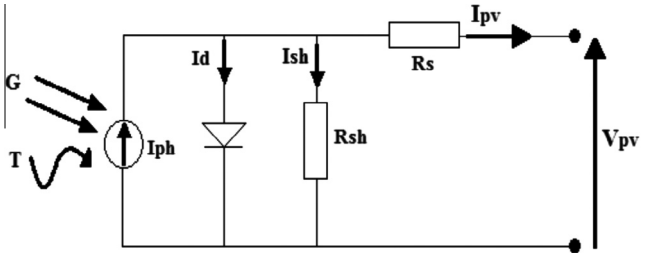

Fig. 1. Equivalent circuit of solar cell.

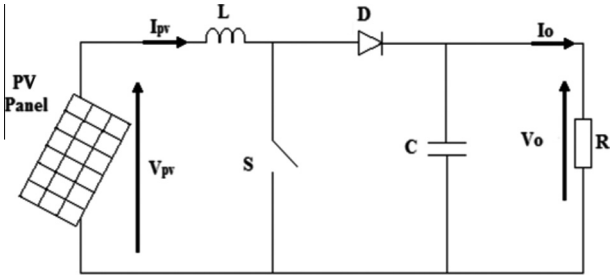

Fig. 3. Power stage schematic of boost converter.

Table 1
Parameter specification of STP080S-12/Bb PV panel.

Parameter	Variable	Value
Maximum power	P_m	80 W
Maximum voltage	V_m	17.5 V
Current at max power	I_m	4. 58 A
Open circuit voltage	V_{oc}	21.9 V
Short circuit current	I_{sc}	4.95 A

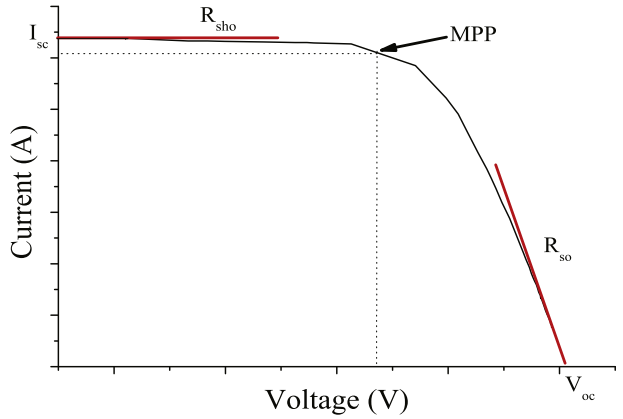

Fig. 2. Experimental Ipv(Vpv) characteristic for a given temperature and solar radiation data.

The accuracy of FOCV and FSCC methods is not guaranteed because they approximate a constant ratio of V_{oc} and V_{mpp} or I_{sc} and I_{mpp}.

To overcome the disadvantages mentioned above a fuzzy logic algorithm and neural network (NN) have been developed [11,12]. In general, the controllers by fuzzy logic can provide an order more effective than the traditional controllers for the nonlinear systems, because there is more flexibility [13]. The main disadvantage of the fuzzy logic controllers is their reliance on the designers knowledge of the system.

Because of this diversity of MPPT methods in the years president researchers and practitioners in PV systems have presented a comparative analysis of existences MPPT techniques [14,15].

In this paper a comparative study of current perturbation algorithm (CPA) and short circuit current (FSCC) MPPT algorithms is presented. To overcome the drawbacks in these two methods a novel MPPT algorithm is proposed.

The real time simulation using dSPACE is carried out in this paper for constant and variable irradiance considering the temperature was kept unchanged during a day.

This paper is organized as follows; Section "Mathematical modeling of PV solar module" descries the PV system modeling. Secti on "DC–DC boost converter" is devoted to the DC–DC boost converter. The MPPT techniques are explained in Section "MPPT techniques". In Section "Configuration and operation of proposed system" configuration and operation of proposed system is presented. Simulation results, analysis and discussion are illustrated in Section "Simulations". Section "Experimental results and discussions" presents the experimental results obtained. Finally conclusions end the paper.

Table 2
Dynamics of perturbation size.

$sign\Delta P_{pv1}$	$sign\Delta P_{pv0}$	$I(k)$
1	1	$\Delta I(k-1)$
1	−1	$m_1\Delta I(k-1)$
−1	1	$m_1\Delta I(k-1)$
−1	−1	$\Delta I(k-1)$

Mathematical modeling of PV solar module

PV modules are made by combining a large number of elementary cells (series and/ or parallel). The equation for the model of the photovoltaic cell involves the relationship between the output voltage, V_{pv}, and the current, I_{pv}. The main equation for a cells output current can be modeled through the circuit shown in Fig. 1 [16].

$$I_{pv} = I_{ph} - I_s * \left[\exp\left\{q\frac{(V_{pv}+R_sI_{pv})}{AkT}\right\} - 1\right] - \frac{V_{pv}+R_sI_{pv}}{R_{sh}} \quad (1)$$

where V_{pv} and I_{pv} represent the output voltage and current of the solar cell, respectively; I_s is the total diffusion current through the PN junction; q is the electron charge ($1.6e^{-19}C$); A is an diode-ideality factor of the PN junction; K is the Boltzmann constant ($1.38e^{-23}J/K$); T is the temperature (K); R_s and R_{sh} is the series and parallel resistance of the cell, respectively.

For the simulation and the experimental setup, the Sun-Tech STP080S-12/Bb module was chosen. The electrical parameters are given in Table 1.

To determine the series, shunt resistance and the ideality factor we used the five parameters method, for a given temperature and solar radiation data according to the open voltage circuit V_{oc}, the short circuit current I_{sc} , the voltage V_m and current I_m to the maximum power point (MPP) and the slopes of the curves I–V near V_{oc} and I_{sc} [17].

Thus, determination of the parameters is given by Eqs. (2)–(6):

$$\left(\frac{dV_{pv}}{dI_{pv}}\right)_{V_{pv}=V_{oc}} = -R_{so} \quad (2)$$

$$\left(\frac{dV_{pv}}{dI_{pv}}\right)_{I_{pv}=I_{sc}} = -R_{sho} \quad (3)$$

$$A = \frac{V_m + (I_m * R_s) - V_{oc}}{V_t\left[ln\left(I_{sc} - \frac{V_m}{R_{sho}} - I_m\right) - ln\left(I_{sc} - \frac{V_{oc}}{R_{sho}}\right) + \frac{I_m}{I_{sc}-\frac{V_{oc}}{R_{sho}}}\right]} \quad (4)$$

$$R_s = R_{so} - \frac{AV_t}{I_s}exp\left(-\frac{V_{oc}}{A*V_t}\right) \quad (5)$$

$$R_{sh} = R_{sho} \quad (6)$$

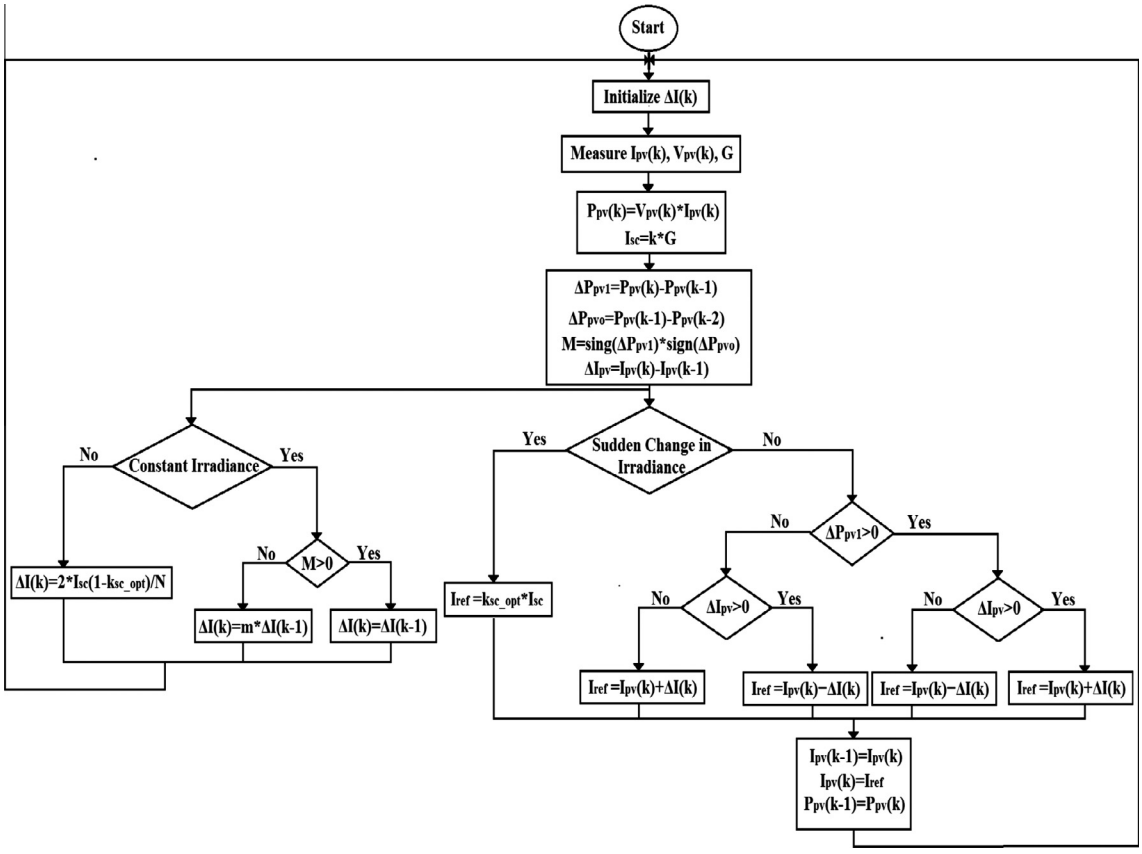

Fig. 4. Flowchart of the proposed MPPT algorithm.

R_{so} and R_{sho} are calculated based on the slopes of the experimental $I_{pv}(V_{pv})$ curves Fig. 2. Different cell parameters change with illumination and the ambient temperature may be approximated by the following equation system.

$$I_{ph} = I_{ph_{nom}}[1 + a(T - T_{nom})] \tag{7}$$

$$I_{ph_{nom}} = I_{sc_{nom}} * \frac{G}{G_{nom}} \tag{8}$$

$$a = \frac{I_{sc}(T_2) - I_{sc}(T_1)}{I_{sc}(T_1)} * \frac{1}{T_2 - T_1} \tag{9}$$

$$I_s = I_{so} * \left(\frac{T}{T_{nom}}\right)^{\frac{3}{A}} * exp\left[\left(-\frac{E_g}{Ak}\right) * \left(\frac{1}{T} - \frac{1}{T_{nom}}\right)\right] \tag{10}$$

$$I_{so} = \frac{I_{sc\_nom}}{exp\left(q\frac{V_{oc\_nom}}{AkT_{nom}} - 1\right.} \tag{11}$$

The terms $G_{nom}, T_{nom}, V_{oc\_nom}$ and I_{sc_nom} are irradiance, temperature, open circuit voltage and short circuit current of PV panel at standard test conditions (STCs), respectively.

The value of R_{sh} impact little on the output characteristics of PV cells, while R_s has a big influence. Therefore, the value of R_{sh} can be neglected.

DC–DC boost converter

A DC/DC boost converter is used in order to optimize the power provided by the PV module, Fig. 3 shows the structure of the boost chopper, where K is the main switch, L is the filter inductor, and C is the filter capacitor, R is the load resistor.

The system dynamics are described by the following equations [18].

$$\frac{dI_{pv}}{dt} = \frac{V_{pv}}{L} - \frac{(1-D)}{L}V_0 \tag{12}$$

$$\frac{dV_0}{dt} = \frac{(1-D)}{C}I_{pv} - \frac{1}{RC}V_0 \tag{13}$$

I_{pv}, V_{pv}, V_0 and D are input current, input voltage, output voltage and duty ratio of boost converter, respectively.

It is assumed that the boost converter is operating in continuous current mode (CCM), when the switch S is in the on state, the current in the boost inductor increases linearly. The diode D is off at the time. When the switch S is turned off, the energy stored

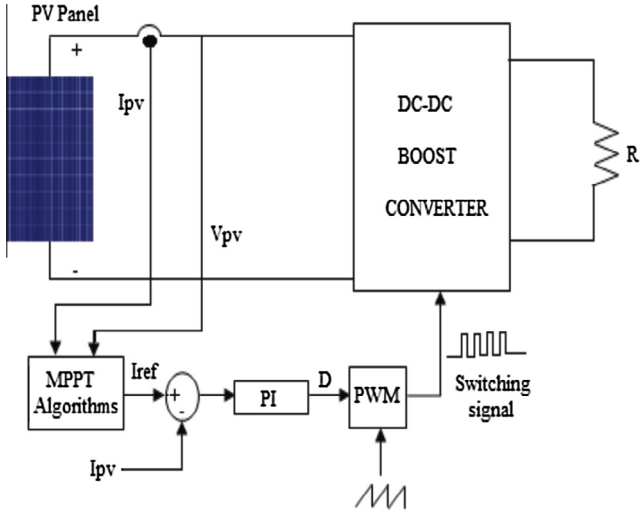

Fig. 5. Blocks diagram illustrating the fundamental structure of the proposed system.

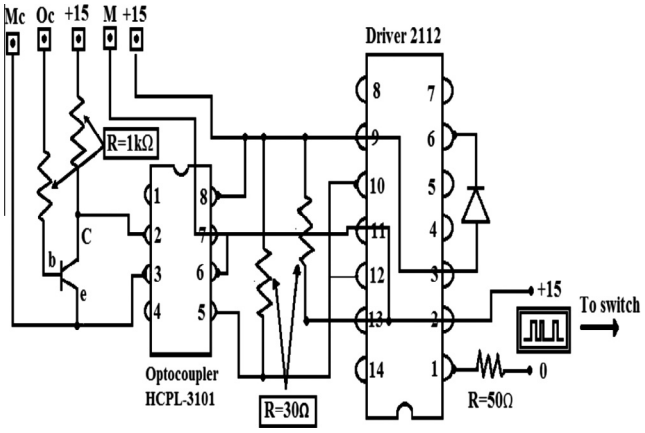

Fig. 6. Galvanic isolation circuit.

in the inductor is released through the diode to the input *RC* circuit [19].

At steady-state operation of the converter, the mean inductor voltage is zero over a full switching period *T*; from this we derive the output voltage.

$$V_0 = \frac{V_{pv}}{1-D} \tag{14}$$

The boost converter operates in the CCM for $L > Lmin$, where:

$$L_{min} = \frac{(1-D)DV_0}{f\Delta I} \tag{15}$$

The minimum value of the filter capacitance that results in the voltage ripple ΔV is given by

$$C_{min} = \frac{DV_0}{Rf\Delta V} \tag{16}$$

Here, f is the switching frequency and R is the load resistance. The relation between the output and the input voltage depend on the duty-cycle. Assuming an efficiency of $\eta = 100\%$ meaning that the converter is a POPI type (Power out = Power in) we obtain the optimum load.

$$R = \frac{V_{pv}}{I_{pv}(1-D)^2} \tag{17}$$

MPPT techniques

Current perturbation algorithm (CPA)

The perturbation and observation (P&O) is probably the most commonly used MPPT algorithm because it is simple and requires only measurements of voltage and current of the photovoltaic panel; it can track the maximum power point even during variations of the irradiance and temperature. As the name suggests the conventional P&O algorithm operate periodically by perturbing

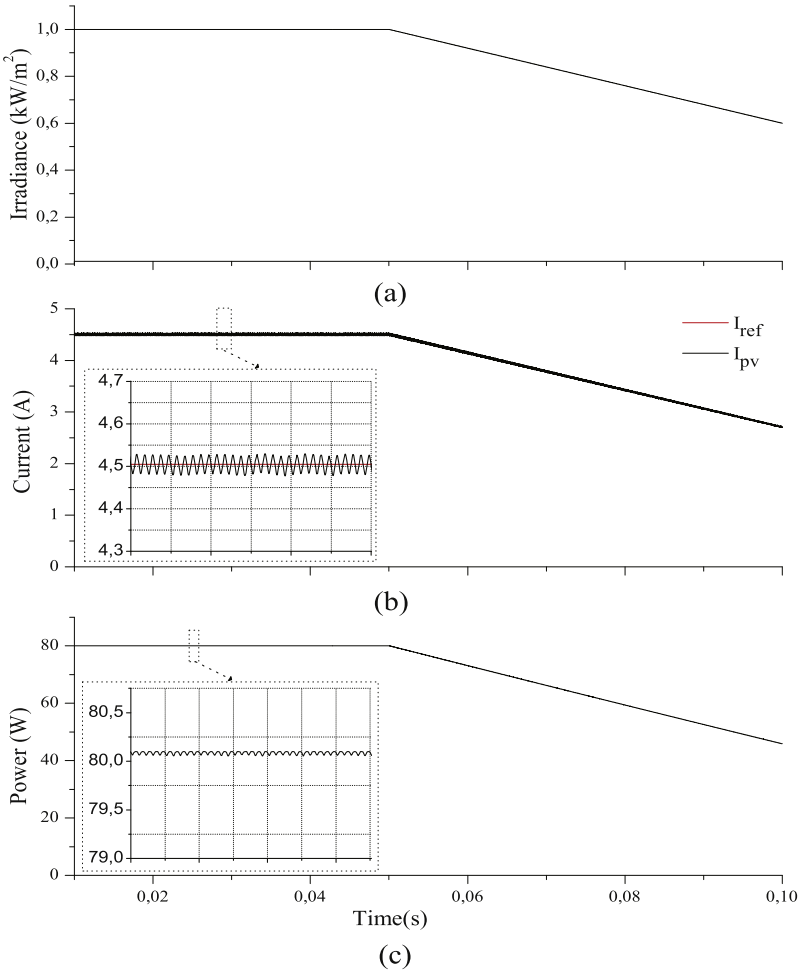

Fig. 7. (a) Solar irradiation, (b) reference and panel current, and (c) panel power using FSCC method.

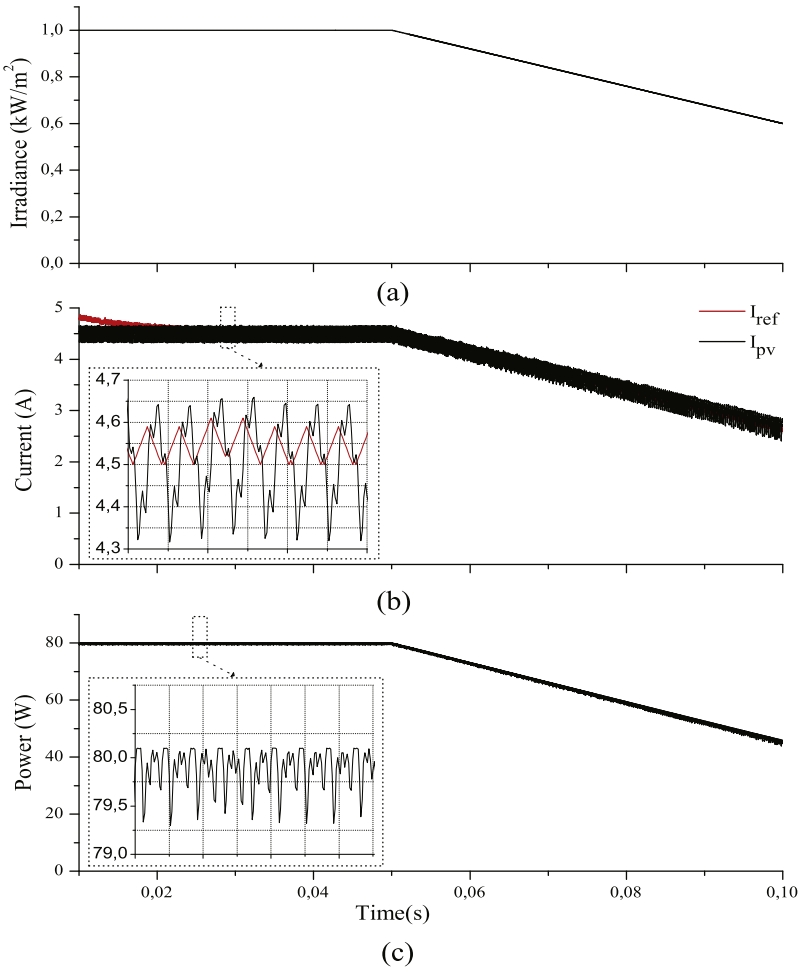

Fig. 8. (a) Solar irradiation, (b) reference and panel current, and (c) panel power using CPA method.

(incrementing or decrementing) the duty cycle of the DC–DC converter and comparing the PV output power with that of the previous perturbation cycle. If the power is increasing the perturbation will continue in the same direction in the next cycle, otherwise the perturbation direction will be reversed [20].

Theoretically, the algorithm is simple to implement in its basic form. However, it was noticed some oscillations around the MPP in steady state operating and this causes power loss.

The current perturbation algorithm (CPA) uses the same concept of a conventional P&O algorithm, but it considers current perturbation. The flowchart of the current perturbation MPPT algorithm is presented in Fig. 4.

$$I_{ref} = I_{pv}(k) + sign(I_{pv}(k) - I_{pv}(k-1)) * sign(P_{pv}(k)) \quad (18)$$

In Fig. 4, $I_{pv}(k), V_{pv}(k)$, and $P_{pv}(k)$ are current, voltage, and power of PV module, respectively.

The fractional short circuit current method (FSCC)

The short circuit current method is one of the simplest offline methods, which uses an approximately linear relationship between the short circuit current (I_{sc}) and the maximum power point current (I_{mpp}) under different environmental conditions. In order to achieve this method, an additional switch is added to the power converter to periodically short circuit the PV source so that I_{sc} can be measured using a current sensor. The MPPT calcu-lated using this technique is based on Eq. (19).

$$I_{mpp} = k_{sc\_opt} * I_{sc} \quad (19)$$

This factor k_{sc_opt} has been reported to be between 0.78 and 0.92. Once the constant k_{sc_opt} is known, I_{mpp} is computed by measuring I_{sc} periodically. Although the implementation of this method is simple and cheap, its efficiency is relatively low due to the utilization of inaccurate values of the constant k_{sc_opt} in the computation of I_{mpp}. FSCC MPPT needs only a current sensor and therefore it is less expensive and easy to implement. The disadvantage includes the periodic loss of power while measuring the short circuit current [21].

Proposed algorithm

The P&O MPPT algorithm works well when the irradiance changes slowly. Two main drawbacks affect P&O-based MPPT in presence of slowly-varying irradiance, the operating point oscillates around the MPP causing loss of energy and, in addition, in presence of rapidly changing atmospheric conditions, the P&O algorithm can be confused. The design of the proposed algorithm is based on the current perturbation algorithm (CPA) given in Eq. (18), where the output current of the solar module operate in the following range.

$$I_m \leqslant I_{pv}(k) \leqslant I_M \quad (20)$$

The maximum and the minimum value of the operating current are defined by Eqs. (21) and (22) respectively.

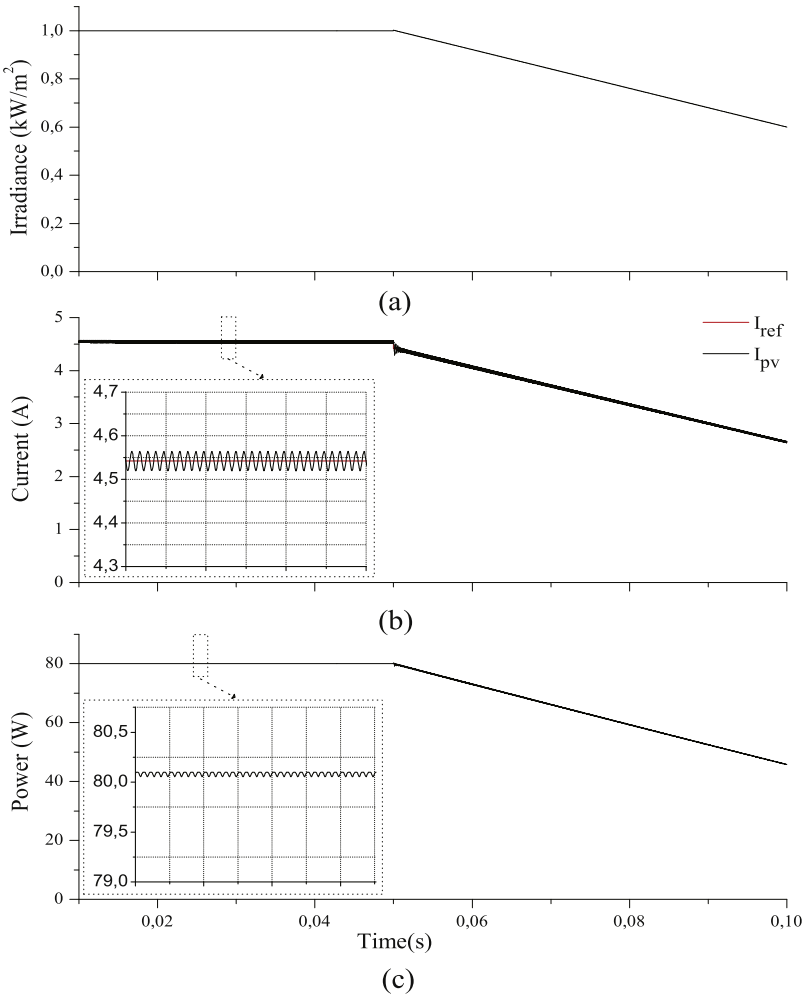

Fig. 9. (a) Solar irradiation, (b) reference and panel current, and (c) panel power using proposed method.

$$I_M = I_{sc} \tag{21}$$

$$I_m = 2I_{mmp} - I_{sc} = 2k_{sc\_opt} \tag{22}$$

A generalized expression is derived also to estimate the short circuit current for changes in irradiance to resolve the problem of the short circuited of the PV panel Eq. (23).

In this paper, a new MPPT algorithm is proposed to reduce the number of oscillations around the MPP in steady state and search very well the MPP under rapidly changing conditions using the advantages of the two algorithms (CPA and FSCC). From Eqs. (7) and (8) the short circuit current can be estimated according to the irradiance, given in

$$I_{sc} = I_{sc\_nom} * \frac{G}{G_{nom}} \tag{23}$$

Therefore, once the irradiance is known the short circuit current can be determined Eq. (23).

The process of the proposed MPPT algorithm is illustrated in the flow chart as presented in Fig. 4, where the perturbation step ΔI is added to the reference current I_{ref} at each iteration of the algorithm and the value of the reference current is determined by one of the two previous algorithms (CPA or FSCC) and that's dependent if the illumination is constant, if there is a slow variation or sudden change in the irradiance.

The determination of $\Delta I(k)$ was taken from the variable perturbation size adaptive P&O MPPT algorithm presented in [4]. The amplitude of the current perturbation is a very important parameter requiring optimization; lowering $\Delta I(k)$ reduces the steady-state losses caused by the oscillation of the array operating point around the MPP. The determination of the variable current perturbation $\Delta I(k)$ depending on the value of the irradiance variation.

$$\Delta I(k) = \frac{I_M - I_m}{N} = \frac{2I_{sc}(1 - k_{sc\_opt})}{N} \tag{24}$$

where N is the maximum number of iterations required to determine MPP.

$$\Delta I(k) = \left(m_1 - m_2 \frac{|M|}{2}\right) \Delta I(k-1) \tag{25}$$

where m_1 is the reduction factor of perturbation size and $m_2 = 1 - m_1$. The variable M accounts for oscillations of operating point around MPP and defined as

$$M = sign\Delta P_{pv1} - sign\Delta P_{pv0}$$

where

$$P_{pv0} = -P_{pv}(k-2) + P_{pv}(k-1)$$

$$P_{pv1} = P_{pv}(k) - P_{pv}(k-1)$$

The perturbation size is reduced by factor m_1, to make the operating point is moving near from the MPP, as shown in Table 2. Finally, if there is a sudden change in irradiance then the FSCC

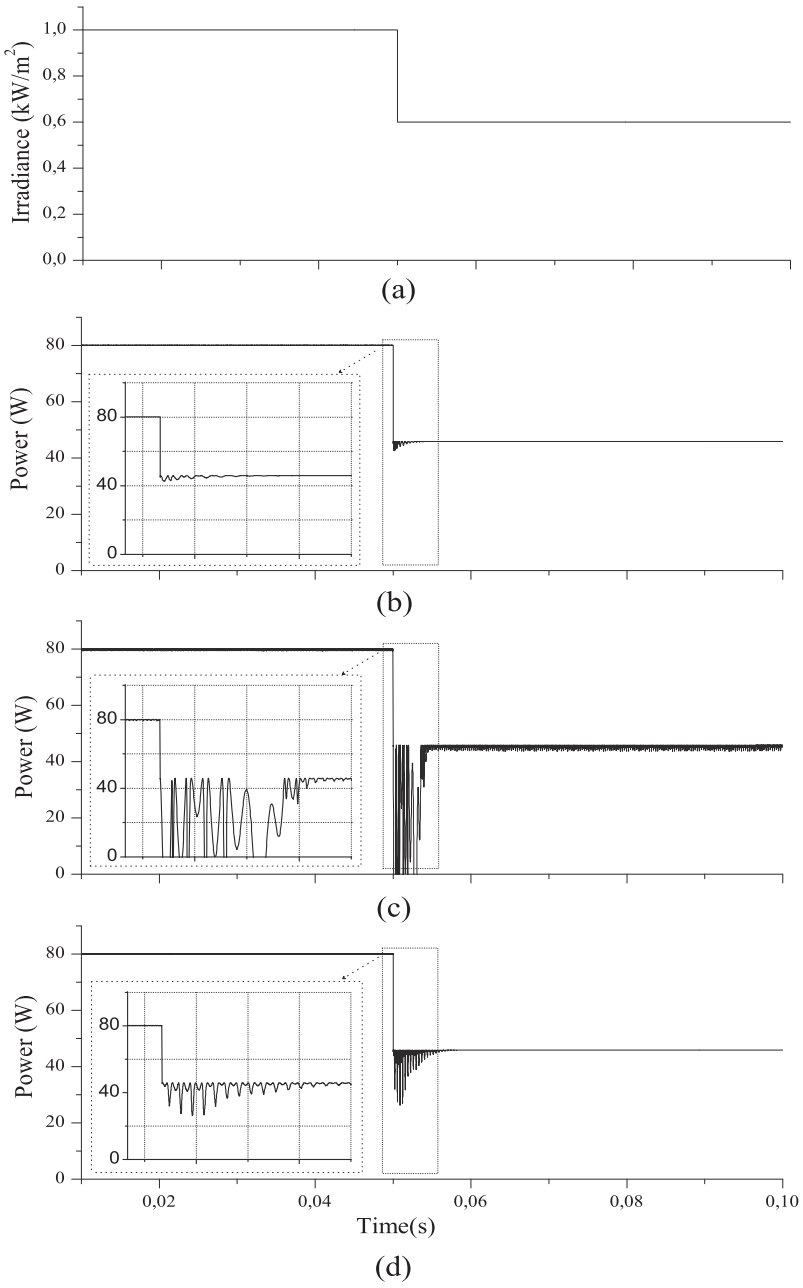

Fig. 10. (a) Solar irradiation, (b) panel power using FSCC method, (c) panel power using CPA method, and (d) panel power using proposed method.

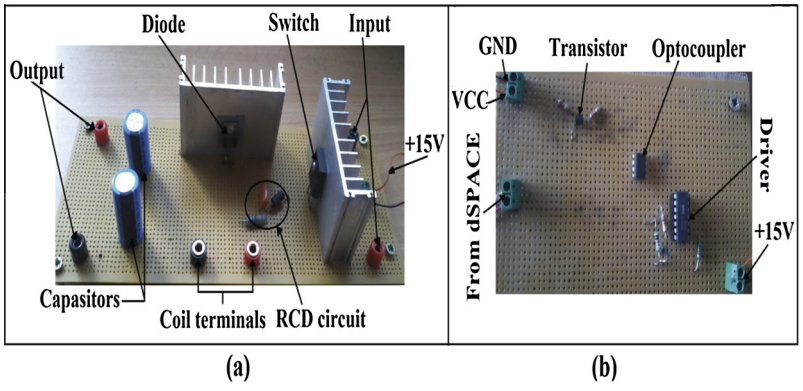

Fig. 11. DC–DC boost converter, (a) power circuit and (b) control circuit.

method is used to determine the reference current and the current perturbation $\Delta I(k)$ is calculated with Eq. (24). Otherwise the reference current is calculated with the CPA method and $\Delta I(k)$ is obtained by Eq. (25).

Configuration and operation of proposed system

A system configuration of the experimental prototype is shown in Fig. 5. A basic topology of the power converter is a current-controlled boost chopper.

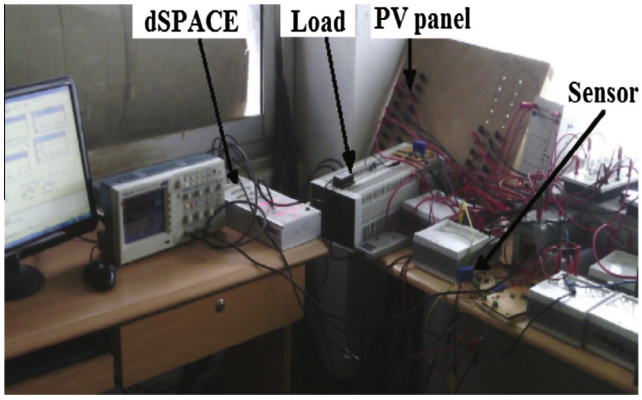

Fig. 12. The experimental used platform.

Let us consider that the boost converter operate at MPP and at standard test conditions STC; $V_{pv} = V_{mpp}, I_{pv} = I_{mpp}$ and for load resistive R of 20 Ω.

To minimize the oscillation at MPP the inductor and the output capacitor values are designed for 1% current ripple ΔI_{pv} and voltage ripple ΔV_{pv} respectively.

A dc current sensor is employed for controlling an average current of the boost converter. The output current of the PV flows through a diode inserted to block a reverse current.

In this system, the optimum operating current is the output of the MPPT algorithms, the difference between the reference current and the output current of the PV panel flows through a proportional and integral (PI) controller and generates a duty cycle to a pulse width modulator (PWM) where the modulation frequency is 20 kHz.

The transfer function of control to panel current is given by [22].

$$G_i(s) = \frac{V_o}{L}\left(s + \frac{2}{RC}\right) * \frac{1}{den(s)} \tag{26}$$

where the denominator polynomial is

$den(s) = s^2 + \frac{1}{RC}s + \frac{(1-D)^2}{LC}$

The transfer function of the PI controller is defined by

$$G_c(s) = \left(k_p + \frac{k_i}{s}\right) \tag{27}$$

The closed-loop transfer function is given by

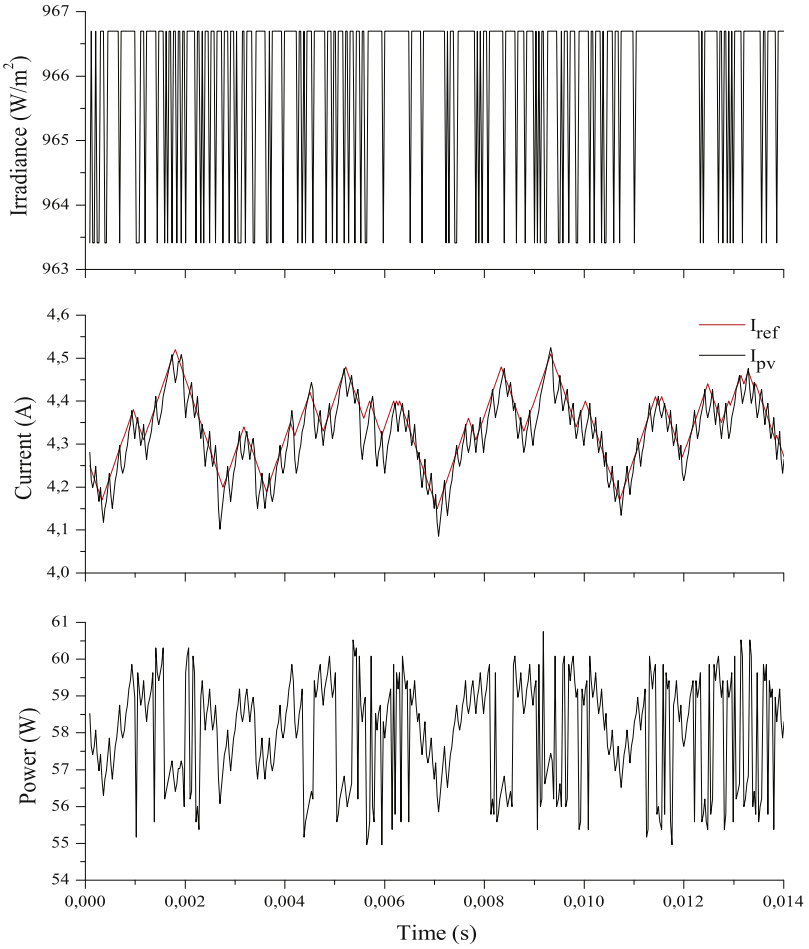

Fig. 13. Experimental results showing the system responses to a PV panel for ($\Delta I = 0.01$).

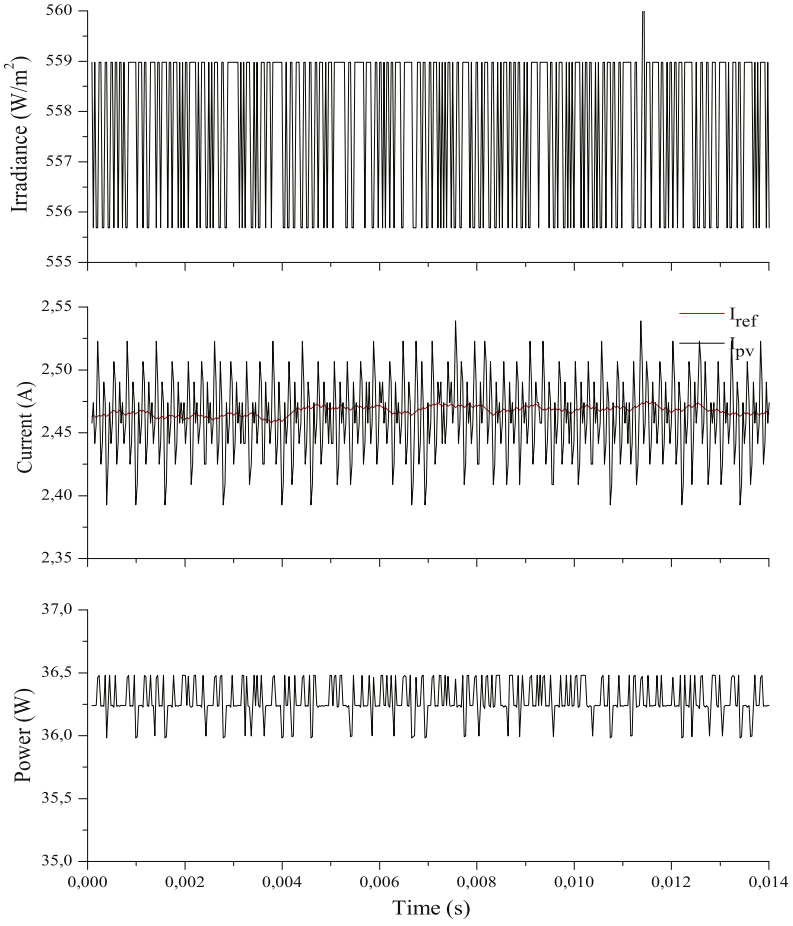

Fig. 14. Experimental results showing the system responses to a PV panel for ($\Delta I = 0.001$).

$$G_{TF}(s) = \frac{G_i(s) * G_c(s)}{1 + (G_i(s) * G_c(s))} \tag{28}$$

Before arriving to the power switch gate, the resulting pulse moves on the galvanic isolation block which separates the control circuit from the power circuit; the galvanic isolation is based on an opto-coupler and a driver Fig. 6.

A transistor operating in the mode 'switching' can transform and amplify the pulse from the dSPACE card to amplitude of 0 and 15 V for controlling the power switch [23].

Simulations

The results of the computer simulation for the FSCC, the CPA and the proposed MPPT algorithm for a fixed temperature (T = 25 °C) and variable irradiance (G) are presented in this section.

The model consists of a PV panel that can be configured to perform with the desired characteristics, a DC–DC boost converter to step up the output voltage of the PV panel to feed the resistive load, MPPT algorithm to determine the operating point and PI controller to regulate the current of the PV panel.

The regulation is achieved by pulse-width modulation (PWM) technique and the switching device is normally MOSFET or IGBT.

Maximum power is reached when the MPPT algorithm changes and adjusts the PWMs duty cycle of the DC–DC boost converter.

The value of inductor is 500 μH and the capacitor is about 47 μF. For the load, resistor is used with value of 20 Ω.

Fig. 7 shows that the FSCC method can obtain the maximum power of the panel without any perturbation if the irradiance is constant or if it's varying slowly, in spite of the absence of the perturbation this method gives some losses in the power because the proportional relationship between the reference current and the short circuit current is an approximation.

Fig. 8 shows that for constant irradiance level, there is a perturbation around the real maximum power point; this perturbation depending on the choice of the value of the current perturbation step applied to the system which is the main factor determining not only the amplitude of oscillations but also the convergence rate to the final response.

From Fig. 9, it is noticed that the proposed MPPT algorithm can track the exact maximum power from the PV panel quickly and accurately without perturbation, hence this last has better performance compared to CPA and FSCC.

To observe the performance of the proposed algorithm, the three MPPT algorithms are verified for sudden changes in irradi-ance through digital simulations Fig. 10. When there is a sudden change in irradiance the current perturbation algorithm loses the control for certain of time which makes very important losses in the panel power, on the other side the proposed algorithm stay works correctly. The proposed MPPT algorithm has better response time, less oscillation and much more accurate tracking at each step.

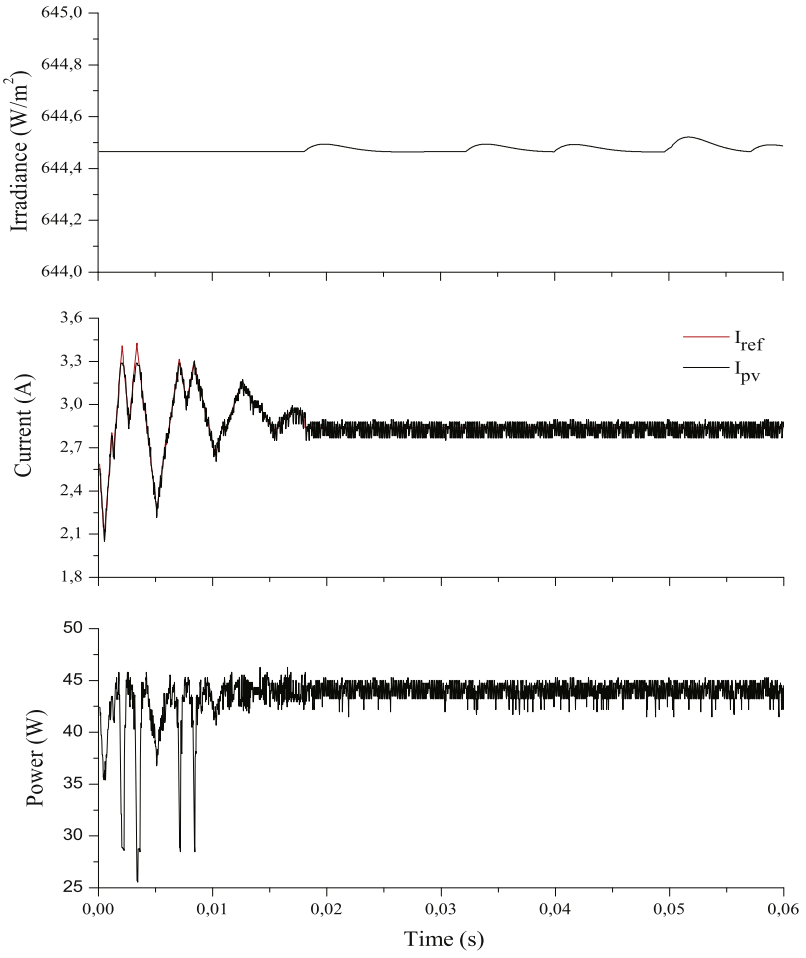

Fig. 15. Experimental results showing the system responses to a PV panel for variable current perturbation ΔI.

Experimental results and discussions

To elaborate this study a STP080S-12/Bb PV panel with angle of 30° has the parameters presented in Table 1 is used. For voltage and current data processing; LEM sensors (LV25-P and LA25-P) were used as inputs to the interface of the dSPACE 1104, the output of the dSPACE is the PWM pulses between 0 and 5 V, thus for amplifying the output voltage to a voltage sufficient to fed the IGBT (15 V) we used an amplifier circuit, when the pulses are amplified they pass by an isolated circuit to separate the power circuit and the control circuit Fig. 11. Low pass filters are used for noise rejection from the array current and voltage feedback signals. The simulation results have been well validated experimentally using dSPACE1104 platform Fig. 12.

The proposed algorithm is implemented in the dSPACE to confirm the simulation results with a real time simulation. For comparison, FSCC method and CPA method are also implemented using the same hardware specification. Using the prototyping cir-cuits, the MPP tracking efficiency tests are carried out.

In the CPA algorithm the amplitude of the perturbation step size applied to the system, is the main factor determining the amplitude of oscillations and hence the convergence rate to the final response. To understand the influence of this factor Figs. 13 and 14 are presented.

From the first graph we can see that the P&O method produce a perturbation around the real MPP which causes a power losses; for exemple in that case the power fluctuate between 54 W and 61 W. We can solve this problem by decreasing of the perturbation size (ΔI) to 0.001 Fig. 14, but this decrease the rate of response of the system and the system can be converged.

A variable current perturbation is applied to obtain an effective way to improve the behavior of stable state performance Fig. 15.

Fig. 15 shows that when we apply a variable current perturbation instead of a fixed current perturbation the perturbation will be decreased after a few seconds which reduce the power losses.

From the previous graphs, it is observed that the proposed algorithm reaches MPP without any perturbation compared with CPA algorithm.

To demonstrate the performance of this algorithm a variable irradiance is applied to the PV panel. From Fig. 16 we can confirm that the proposed algorithm works very well not only if the irradiance is constant but also for a variable irradiance.

Conclusion

In this work a novel MPPT method has been developed, in order to overcome the problems of the conventional P&O MPPT technique. The concept of the proposed algorithm is based on the FSCC (Fractional Short Circuit Current) and CPA (Current Perturbation Algorithm) methods. To improve the efficiency of the proposed algorithm a comprehensive analysis and experimental evaluation of three MPPT algorithms is presented in this study. The effects of the perturbation step size of the P&O MPPT algorithm on the system behavior were also examined.

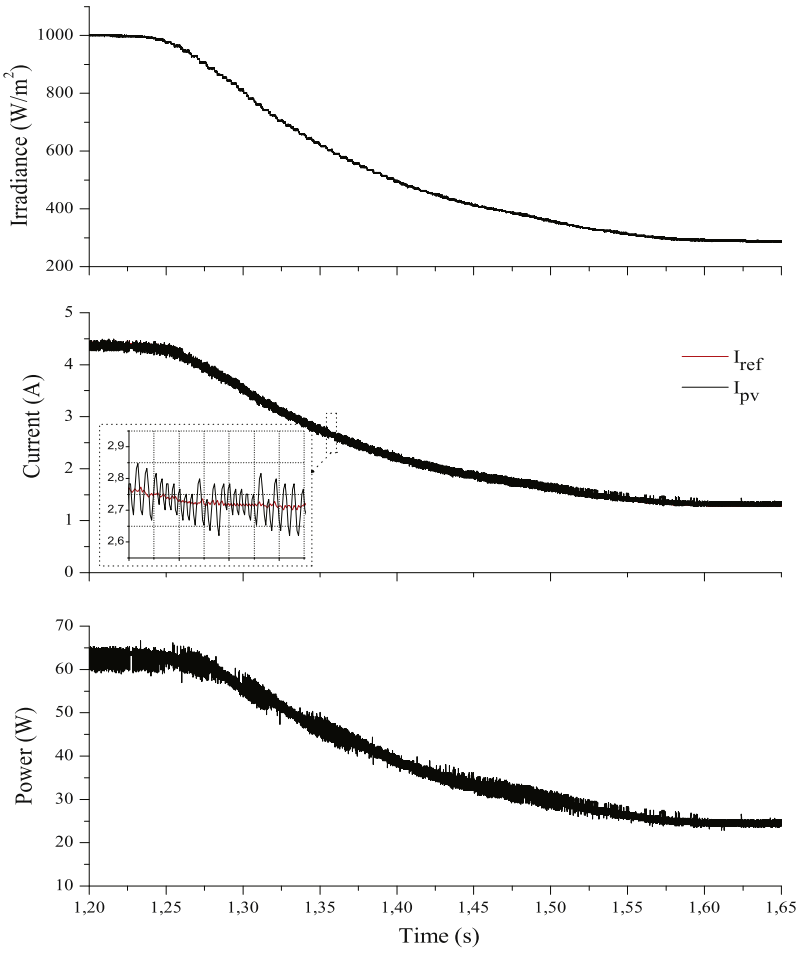

Fig. 16. Experimental results of the proposed MPPT for variable irradiance.

Unlike the classic P&O MPPT algorithm, the proposed algorithm has a faster response and capability of reduces the steady state oscillation and eliminates the probability of divergence form the MPP locus under both static and dynamic conditions.

References

[1] Pandey Ashish, Dasgupta Nivedita, Mukerjee Ashok Kumar. High-performance algorithms for drift avoidance and fast tracking in solar MPPT system. IEEE Trans Energy Convers 2008;23(2). June.

[2] Bianconi Enrico, Calvente Javier, Giral Roberto, Mamarelis Emilio, Petrone Giovanni, Ramos-Paja Carlos Andrs, et al. Perturb and observe MPPT algorithm with a current controller based on the sliding mode. Electr Power Energy Syst 2013;44:346356.

[3] Wua Yu-Chi, Chen Meng-Jen, Huang Sih-Hao, Tsai Ming-Tsung, Li Chia-Huang. Maximum power point tracking on stand-alone solar power system: three-point-weighting method incorporating mid-point tracking. IEEE Electr Power Energy Syst 2013;52:1424.

[4] Kollimalla Sathish Kumar, Mishra Mahesh Kumar. Variable perturbation size adaptive P&O MPPT algorithm for sudden changes in irradiance. IEEE Trans Sust Energy 2014;5(3). July.

[5] Elgendy Mohammed A, Zahawi Bashar, Atkinson David J. Assessment of perturb and observe MPPT algorithm implementation techniques for PV pumping applications, power delivery. IEEE Trans Sust Energy 2012;3(1). January.

[6] Sera Dezso, Mathe Laszlo, Kerekes Tamas, Spataru Sergiu Viorel, Teodorescu Remus. On the perturb-and-observe and incremental conductance MPPT methods for PV systems. IEEE J Photovoltaics 2013;3(3). July.

[7] Zoua Yinqing, Yua Youling, Zhangb Yu, Luc Jicheng. MPPT control for PV generation system based on an improved inccond algorithm. 2012 International workshop on information and electronics engineering, vol. 29. p. 105–9.

[8] Masoum Mohammad AS, Dehbonei Hooman, Fuchs Ewald F. Theoretical and experimental analyses of photovoltaic systems with voltage- and current-based maximum power-point tracking. IEEE Trans Energy Convers 2002;17(4). December.

[9] Noguchi Toshihiko, Togashi Shigenori, Nakamoto Ryo. Short-current pulse-based maximum-power-point tracking method for multiple photovoltaic-and-converter module system. IEEE Trans Ind Electron 2002;49(1). February.

[10] Parlak Koray Sener. FPGA based new MPPT (maximum power point tracking) method for PV (photovoltaic) array system operating partially shaded conditions. Energy 2014;68:399e410.

[11] Algazar Mohamed M, AL-monier Hamdy, EL-halim Hamdy Abd, Salem Mohamed Ezzat El Kotb. Maximum power point tracking using fuzzy logic control. Electr Power Energy Syst 2012;39:2128.

[12] Rai Anil K, Kaushika ND, Singh Bhupal, Agarwal Niti. Simulation model of ANN based maximum power point tracking controller for solar PV system. Solar Energy Mater Solar Cells 2011;95:773778.

[13] Bounechba H, Bouzid A, Nabti K, Benalla H. Comparison of perturb & observe and fuzzy logic in maximum power point tracker for PV systems. The international conference on technologies and materials for renewable energy, environment and sustainability, TMREES14. Energy procedia 2014;50:677–84.

[14] de Brito Moacyr Aureliano Gomes, Galotto Luigi, Sampaio Leonardo Poltronieri, de Azevedo e Melo Guilherme, Canesin Carlos Alberto. Evaluation of the main MPPT techniques for photovoltaic applications. IEEE Trans Ind Electron 2013;60(NO. 3). March.

[15] Esram Trishan, Chapman Patrick L. Comparison of photovoltaic array maximum power point tracking techniques. IEEE Trans Energy Convers 2007;22(2). June.

[16] Koutroulis Eftichios, Kalaitzakis Kostas, Voulgaris Nicholas C. Development of a microcontroller-based, photovoltaic maximum power point tracking control system. IEEE Trans Power Electron 2001;16(1). January.

[17] Chan Danel SH, Phang Jacob CH. Analytical methods for the extraction of solar-cell single- and double-diode model parameters from I–V characteristics. IEEE Trans Electron Dev 1987;ed-34(2). February.

[18] Chu Chen-Chi, Chen Chieh-Li. Robust maximum power point tracking method for photovoltaic cells: a sliding mode control approach. Sol Energy 2009;83:13701378.

[19] Muhammad H Rashid. Power electronics handbook devices, circuits, and applications, 3rd ed.

[20] Ahmed Jubaer, Salam Zainal. An improved perturb and observe (P&O) maximum power point tracking (MPPT) algorithm for higher efficiency. Appl Energy 2015;150:97108.
[21] Sher Hadeed Ahmed, Murtaza Ali F, Noman Abdullah, Addoweesh Khaled E, Chiaberge Marcello. An intelligent control strategy of fractional short circuit current maximum power point tracking technique for photovoltaic applications. J Renew Sust Energy 2015;7:013114.
[22] Jin Yanyan, Xu Jianping, Zhou Guohua, Mi Changbao. Small-signal modeling and analysis of improved digital peak current control of boost converter. In: Power electronics and motion control conference, 2009. IPEMC '09. IEEE 6th international.
[23] Bouteldja O. Prédétermination des Caractéréstique d'un Système PV Raccordé au Réseau, Master thesis. Departement of electrotechnics, University Constantine 1, Constantine, Algeria; June 2013.